

Chiral Transition of N=4 Super Yang-Mills with Flavor on a 3-Sphere

Andreas Karch¹ and Andy O'Bannon¹

¹ *Department of Physics, University of Washington,
Seattle, WA 98195-1560*

E-mail: karch@phys.washington.edu, ahob@u.washington.edu

Abstract

We use the AdS/CFT correspondence to perform a numerical study of a phase transition in strongly-coupled large- N_c $\mathcal{N} = 4$ Super-Yang-Mills theory on a 3-sphere coupled to a finite number N_f of massive $\mathcal{N} = 2$ hypermultiplets in the fundamental representation of the gauge group. The gravity dual system is a number N_f of probe D7-branes embedded in $AdS_5 \times S^5$. We draw the phase diagram for this theory in the plane of hypermultiplet mass versus temperature and identify for temperatures above the Hawking-Page deconfinement temperature a first-order phase transition line across which the chiral condensate jumps discontinuously.

1 Introduction

The AdS/CFT correspondence [1] equates the low-energy effective theory of string theory, supergravity (SUGRA), on the background $AdS_5 \times S^5$ with strongly-coupled $\mathcal{N} = 4$ $SU(N_c)$ super-Yang-Mills theory (SYM) in the large- N_c limit living, in some sense, on the boundary of AdS_5 . At finite temperature this four-dimensional boundary is $S^1 \times S^3$. This field theory contains only adjoint fields and exhibits a first-order deconfinement transition at the Hawking-Page temperature, corresponding to AdS-Schwarzschild black hole condensation [2]. The thermodynamics of this SYM theory has been studied in great detail both at strong coupling via AdS/CFT and at zero [3] and weak coupling [4].

Why consider a theory on a compact space? For this conformal theory, the deconfinement transition cannot occur in infinite volume, i.e. on spacetime $S^1 \times \mathbb{R}^3$ because with no scale nothing can set a transition temperature. The S^3 introduces a new scale, and indeed the deconfinement transition occurs at a temperature of order the inverse S^3 radius [4]. On the gravity side, this is the statement that the Hawking-Page transition is only apparent in global AdS coordinates. Poincare patch coordinates are limited to the high-temperature black hole solution, corresponding to the deconfined phase in the SYM theory. Of course, no phase transitions can occur with a finite number of degrees of freedom, which then motivates the 't Hooft limit.

In large- N_c Yang-Mills, or more generally in gauge theories with only adjoint fields, the deconfinement transition comes from order N_c^2 dynamics. One way to identify the deconfinement transition is to ask whether the order N_c^2 contribution to the free energy is zero or not. In pure Yang-Mills, for example, at sufficiently low temperature this contribution to the free energy will be zero, as the degrees of freedom are color singlet glueballs of whom there are order N_c^0 (in the large- N_c book-keeping), while at sufficiently high temperature it will be nonzero, indicating that the contributing degrees of freedom are deconfined gluons of which there are order N_c^2 . This is what the word “deconfinement” means in the $\mathcal{N} = 4$ SYM theory on a 3-sphere studied at strong coupling using AdS/CFT.

Introducing fundamental fields into this field theory requires introducing an open string sector. In reference [5] D7 flavor branes were introduced to the usual AdS/CFT construction, which equates the field theory on a stack of coincident D3-branes with gravity in the geometry supported by the 3-branes. Keeping the number N_f of D7's finite while taking the number N_c of D3's to infinity will produce in the near-horizon limit probe D7-branes embedded in $AdS_5 \times S^5$. These branes will wrap the AdS_5 and an S^3 inside the S^5 factor. The probe branes break half the supersymmetry.

In the field theory this corresponds to adding to the $\mathcal{N} = 4$ theory a number N_f of $\mathcal{N} = 2$ hypermultiplet fields (henceforth “hypers”) in the fundamental representation of $SU(N_c)$. The theory will remain conformal in this $N_f/N_c \rightarrow 0$ limit. The hypers can be given a mass by “ending” the D7-branes at some finite value of the AdS radius [5]. Such masses obviously

break the conformality but will preserve the $\mathcal{N} = 2$ supersymmetry. On the gravity side this is manifest as supersymmetric probe D7's ending at finite radial coordinate, which clearly breaks the radial isometry.

The addition of fundamental fields introduces the possibility of a chiral phase transition analogous to that in quantum chromodynamics (QCD) or at least large- N_c QCD. By the usual large- N_c counting rules, all dynamics of fundamental fields is suppressed by a factor of $1/N_c$. For large- N_c theories, then, the chiral transition involving fundamental fields is in some sense a small perturbation, suppressed by a power of N_c , on top of the order N_c^2 dynamics of the deconfinement transition.

We now review the chiral phase transition in QCD, to compare and contrast with our $\mathcal{N} = 2$ supersymmetric theory on a compact space. We will be careful about two limits: large- N_c and zero quark mass. In general (any N_c and N_f), for massless quarks chiral $U(N_f)_L \times U(N_f)_R \simeq SU(N_f)_L \times SU(N_f)_R \times U(1)_B \times U(1)_A$ is an exact symmetry of the Lagrangian. At zero temperature, $SU(N_f)_L \times SU(N_f)_R$ is spontaneously broken to the diagonal $SU(N_f)_V$. The chiral symmetry is restored at sufficiently high temperatures. The order parameter for the chiral transition is the quark bilinear condensate, which is nonzero at low temperatures and zero at high temperatures, signaling the chiral symmetry restoration. Quark masses explicitly break the chiral symmetry, but we will follow the convention of calling the quark bilinear condensate an order parameter nonetheless.

In QCD with massless quarks, the order of the chiral transition depends on N_c and N_f . We start with $N_c = 3$. For $N_f \geq 3$ massless quarks, universality arguments indicate that the chiral transition is first order [6]. For $N_f = 2$, the chiral transition is believed to be second order [7, 8]¹. For $N_f = 1$, things are more subtle. Now the symmetry is simply $U(1)_B \times U(1)_A$ and the question becomes whether the axial symmetry, which is anomalous at $T = 0$, is restored as the temperature rises. The instantons responsible for the anomaly are suppressed as T rises, so in fact the axial symmetry is believed to be restored at least in the strict $T = \infty$ limit. As the decrease in the density of instantons is believed to be smooth, no chiral transition exists for $N_f = 1$ [6] as a function of T . Turning to the large- N_c limit, for $N_f \geq 2$ the theory has no stable IR fixed point and hence the transition must be first order [6]. At large N_c , the axial anomaly is suppressed and to our knowledge it is not known whether there is a phase transition for $N_f = 1$ and if so at what order. For the theory we are studying the relevant chiral symmetry is also $U(1)_B \times U(1)_A$, so it is precisely this $N_f = 1$, large N_c case that is closest to the supersymmetric theory we have control over. The same symmetry also governs a single staggered fermion in the strong coupling limit. Lattice results for that theory [11] indicate a second order transition.

Next we wish give the quarks nonzero masses and ask what happens to the deconfinement

¹Lattice simulations have not settled the issue of the order of the transition for $N_f = 2$. As just a small sample: [9] found results consistent with a second order transition while more recently [10] found indications of a first order transition

and chiral phase transitions as we dial the mass. Dialing quark masses is not possible in nature but is possible on the lattice, hence we turn to lattice results although we will only present them schematically. The phase diagram for $N_C = 3$ and $N_f = 2 + 1$, is shown in fig. 1 (a.) [12]. Here 2+1 means the quark masses are held at fixed ratios $m = m_u = m_d = r m_s$ for some $r < 1$. What appears are two lines of first-order phase transitions, each ending in a critical point. The lower line is that of chiral transitions, ending in the point C; the upper is the line of deconfinement transitions, ending in the point D.

The chiral transition is identified by a discontinuous jump in the chiral condensate. Only on the $m = 0$ axis, where the chiral symmetry really is a symmetry, is this a genuine symmetry breaking transition.

The deconfinement transition is identified by a discontinuous jump in the Polyakov loop, which is the time-ordered exponential of the holonomy of the gauge field around the time circle. This measures the response of the system to an infinitely massive source of color charge (a quark), and may be written

$$\langle \Omega(x) \rangle = \langle \text{tr} P \exp(i \int d\tau A_0) \rangle \sim \exp(-\Delta F/T) \quad (1.1)$$

where ΔF is the difference in free energy between two equilibrium states, one with an infinitely massive test quark and one without. For pure glue in the confined phase this difference is infinite and hence $\langle \Omega \rangle = 0$. One can think of this as the statement that the color flux lines from the test quark have no place to end except infinity and hence because the flux lines have finite energy density the total energy is infinite. In the deconfined phase, the flux lines are screened, hence $\langle \Omega \rangle$ is finite. Adding dynamical quarks, massive or otherwise, changes this since now flux lines from the test quark have someplace to end. In other words, with dynamical quarks $\langle \Omega \rangle$ is always nonzero, although it may still jump discontinuously. Only in the $m \rightarrow \infty$ limit where the quarks decouple is the pure glue story recovered.

In summary, both order parameters are nonzero everywhere on the interior of fig. 1 (a.). At $m = \infty$ where the quarks decouple, the deconfinement transition occurs at roughly $T_d \sim \Lambda_{QCD} \sim 175 \text{MeV}$. Similarly, for $m = 0$ where the chiral symmetry is an exact symmetry of the Lagrangian, the chiral transition must occur at the same scale (that then being the only scale in the theory). The horizontal line of realistic quark masses falls between points C and D, hence a smooth crossover rather than a phase transition is expected in the real world.

Now we consider the same diagram but with $N_c \rightarrow \infty$, N_f finite. The answer, again only qualitative, is depicted in fig. 1 (b.). The deconfinement transition, being order N_c^2 , does not care about the quark masses and is simply a vertical line. We have drawn the chiral transition line the same way although in principle this need not be the case. Large- N_c arguments indicate that the chiral condensate is independent of T in the confining phase [13, 14] and hence the chiral transition must occur at a temperature $T_{ch} \geq T_d$, we have thus

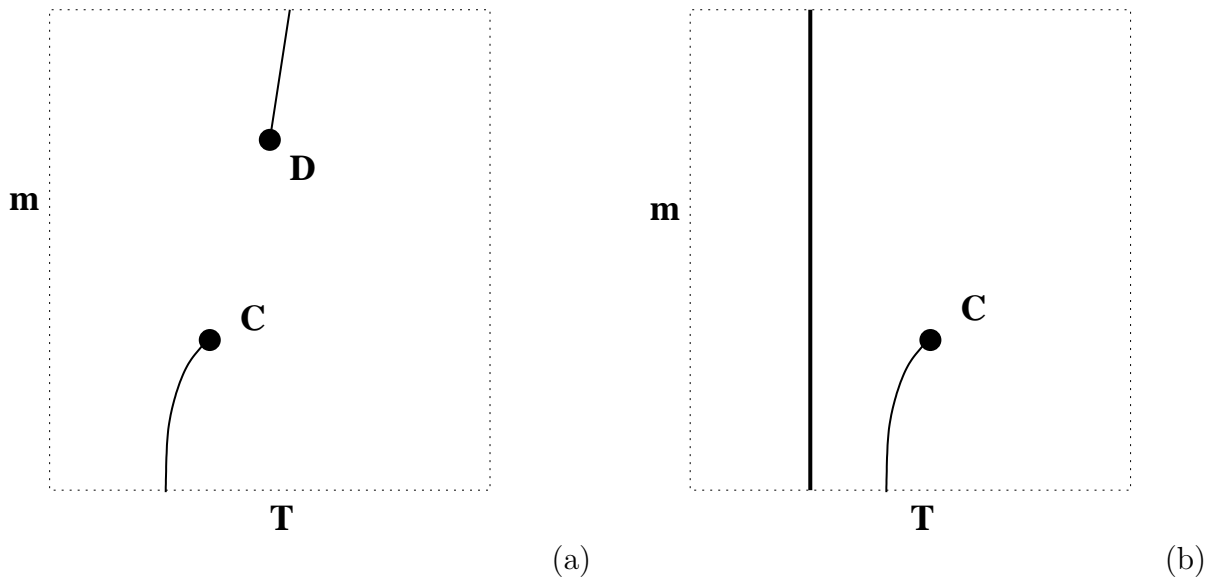


Figure 1: (a.) Phase Diagram of QCD with $N_c = 3$, $N_f = 2 + 1$ (b.) $N_c \rightarrow \infty$, $N_f = 2 + 1$

drawn the deconfinement line to the left of the chiral transition.

In this paper we study the chiral transition in a theory that is in some sense simpler than QCD: large- N_c $\mathcal{N} = 2$ SYM on a 3-sphere. At zero temperature and zero mass, conformal invariance precludes a nonzero chiral condensate, but finite temperature and finite mass both break conformal invariance. We will draw the phase diagram for this theory in the plane of hyper mass versus temperature, identifying the line of a first-order chiral phase transition, which occurs only in the deconfined phase, i.e. above the Hawking-Page temperature. This transition is, in strict thermodynamic terms, not a chiral symmetry breaking transition, but the chiral condensate does jump by a finite amount so for simplicity we will refer to it as a chiral transition. In contrast to QCD we will see that chiral symmetry is unbroken for zero mass at all temperatures, so the deconfinement transition does not come with a standard chiral symmetry breaking transition. Another key difference from QCD will be an independence on the number N_f . Where the order of the chiral transition in QCD depended on N_f , in our theory it is first order for any finite N_f such that $N_f/N_c \rightarrow 0$. The $\mathcal{N} = 2$ Lagrangian explicitly breaks the non-abelian chiral symmetry down to its vector subgroup due to a Yukawa coupling, so the chiral symmetry breaking we are analyzing is a breaking of $U(1)_A \times U(1)_B$ down to $U(1)_B$ as in $N_f = 1$ QCD.

The thermodynamics of large- N_c $\mathcal{N} = 4$ SYM on a 3-sphere at zero 't Hooft coupling, but with a Gauss' law constraint requiring color singlet states, was studied by Sundborg [3], who found that the deconfinement transition was first order. Aharony et. al. [4] studied the same theory at small but finite coupling and found that the deconfinement transition could be either a single first-order transition or two continuous transitions. For pure Yang-Mills on

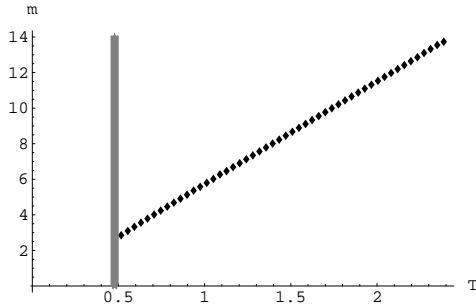


Figure 2: The phase diagram for flavored $\mathcal{N} = 4$ Super-Yang Mills on a sphere as a function of temperature and hyper mass.

a 3-sphere, the former scenario was shown to be the right one [15]. Schnitzer [16] introduced flavor but with N_f/N_c finite, finding that the deconfinement transition becomes third order.

The chiral transition of the D3-D7 system for the $\mathcal{N} = 2$ theory in flat space was studied in [17, 18]. A first-order transition was found [18, 19]². A similar phase transition was also observed for flavor branes in the supergravity dual of confining gauge theories [20]. The phase diagram must by conformality be linear: the quark mass is the only scale that can set a transition temperature. As we will argue below, this infinite volume result can be interpreted as a high-temperature result for the theory on the 3-sphere, and indeed we will find a straight line at high temperatures, providing a useful check of our methods.

Our final result for the chiral transition is the phase diagram in figure (2). The vertical line is the Hawking-Page deconfinement temperature, $T_{HP} = 3/2\pi$ (in units where the AdS radius is one), which comes from order N_c^2 dynamics and is independent of the quark mass. Below T_{HP} , the flavor brane action is independent of temperature, hence whatever occurs at $T = 0$ can be extended up to T_{HP} . This is consistent with the large- N_c field theory arguments that the chiral condensate is independent of temperature in the confining phase [13, 14]. We find no first-order phase transition as a function of temperature below T_{HP} . This comes as a surprise since at zero temperature we see a topology change for the D7 brane as a function of mass.

Above T_{HP} , the flavor brane action depends on the temperature via the presence of the black hole horizon. In this temperature regime, the chiral condensate and free energy exhibit behavior characteristic of a first order transition as m increases, i.e. the first derivative of the

²While we were finishing this manuscript two papers appeared which also reanalyzed the phase transition in this theory, [21] and [22]. In both papers the picture of a first order phase transition as found in [18, 19] is confirmed. Like us, they simplify the numerics by integrating outward instead of shooting inward. In addition [21] argues that when the flavor brane touches the horizon the probe action acquires a new scaling symmetry and a self-similar structure. Their general analysis of Dp/Dq systems corresponding to large- N_c , (p+1)-dimensional thermal gauge theory in infinite volume with fundamental matter confined to a (q+1)-dimensional defect also shows that such phase transitions must be first order. Our results are an extension of this since we consider finite volume and find again a first-order transition in the deconfined phase.

free energy is discontinuous and so on. We have drawn the first-order chiral transition line. Below T_{HP} , the chiral condensate smoothly changes, as does the free energy, as $m \rightarrow \infty$, so we draw no first-order transition line. Everywhere on the $m = 0$ axis, we find numerically that the chiral condensate is zero.

This paper is organized as follows. In section 2 we review the inclusion of flavor branes into the $\mathcal{N} = 4$ theory and identify the chiral symmetry in this theory and its order parameter. In section 3 we write down the probe brane action and counterterms, explain how we extract the condensate and free energy using holographic renormalization, and explain the boundary conditions for our numerics. In section 4 we reproduce known results in infinite volume. In section 5 we present numerical results for the embeddings, condensate, free energy and finally for the phase diagram in the finite volume case. We conclude in section 6 with possibilities for extensions of this study.

2 Adding Flavor to AdS/CFT

We will now describe our system in greater detail, clarifying both the D-brane construction and the symmetries of the boundary theory. The AdS/CFT construction starts with a stack of coincident D3-branes in flat ten-dimensional space in the limit where the number of D3-branes, N_c , goes to infinity and the spacetime in the near-horizon limit becomes $AdS_5 \times S^5$. The limit of zero string length $\alpha' \rightarrow 0$ then decouples open and closed strings, resulting in the now-standard correspondence between the low-energy effective theory of closed strings, ten-dimensional supergravity (SUGRA) in this background, and the low-energy effective theory of open string modes on the D3 worldvolume, $\mathcal{N} = 4$ super-Yang-Mills (SYM) theory in four dimensions in the large- N_c , strong 't Hooft coupling regime. This four-dimensional conformal field theory (CFT) will “live” in a spacetime with the topology of the AdS_5 boundary. Our interest here is in global thermal AdS (and AdS -Schwarzschild) coordinates, with boundary topology $S^1 \times S^3$, which we will call the “curved case”, in distinction to the infinite-volume “flat case”, that is, Poincare patch coordinates with boundary topology $S^1 \times R^3$. We will use the limit of infinite volume to check our methods against known flat case answers.

Thermal AdS is believed to undergo a first-order phase transition [23, 2] called the Hawking-Page transition. At low temperatures the picture is of thermal radiation in equilibrium with itself (assuming perfectly reflecting boundary conditions at the AdS boundary), whereas when the temperature rises the spacetime undergoes a topology change to the AdS-Schwarzschild solution, or in other words a black hole condenses. This transition is only apparent in global AdS coordinates, while the flat case is strictly in the high-temperature black hole phase.

In the dual $\mathcal{N} = 4$ SYM boundary theory, the Hawking-Page transition corresponds to a large- N_c deconfinement transition. “Deconfinement” here means the spontaneous breaking

of the center symmetry and the associated behavior of that symmetry's order parameter, the Polyakov loop, which jumps discontinuously (from zero to nonzero) as the temperature rises. This transition is only apparent for the theory on a compact space, where the inverse S^3 radius can set a transition temperature.

In fact, the ratio of the S^1 and S^3 radii is the only meaningful number so long as the theory is conformal. Letting R_1 be the S^1 radius (inversely proportional to the temperature) and R_3 be the S^3 radius, the infinite-volume limit $R_1/R_3 \rightarrow 0$ is equivalent to the infinite-temperature limit in which $R_1 \rightarrow 0$. In this sense we can compare our finite-volume results, at high-*temperature*, with known infinite-*volume*, finite-temperature results.

Introducing D7-branes orthogonal to the initial D3's in four directions introduces new open string degrees of freedom in the D3 worldvolume theory, from D3-D7 strings, and breaks half the supersymmetry. We will denote the number of D7's as N_f . The so-called probe limit consists of keeping N_f fixed as $N_c \rightarrow \infty$. In this limit, the backreaction of the D7's on the geometry is negligible and hence the result in the near-horizon limit is N_f probe D7-branes embedded in $AdS_5 \times S^5$. From the field theory perspective, knowing that the $\mathcal{N} = 4$ supersymmetry must be broken to $\mathcal{N} = 2$ and from Chan-Paton factors of D3-D7 strings, one can argue that this corresponds to adding matter in the fundamental representation of the gauge group to the $\mathcal{N} = 4$ theory. Specifically, a number N_f of flavors in the form of $\mathcal{N} = 2$ hypers have been added.

From the field theory point of view, these hypers may be massive without breaking supersymmetry although of course this will break conformal invariance. This is manifest in the dual brane picture. In this setup, the D7 wraps all of AdS_5 as well as a trivial cycle inside the S^5 , namely an S^3 . A stable "slipping mode" then exists, which is simply a scalar field on the worldvolume of the D7 that depends only on the AdS_5 radial coordinate [5]. The S^3 that the D7 wraps inside the S^5 may "slip off" the S^5 , as allowed by topology, i.e. contract to a point. If this occurs at a finite value of the radial coordinate, the hyper in the field theory can be shown to have a nonzero mass. The zero mass conformal case is then simply a D7 wrapping the same equatorial S^3 for all values of the radial coordinate.

Indeed, via the AdS/CFT dictionary [5], this scalar slipping mode encodes both the mass of the hyper and the chiral condensate as a function of the mass, as we show below. The key observation is that the D7 worldvolume scalar has a mass (as a scalar in AdS_5) of $m^2 = -3$ (negative but above the Breitenlohner-Freedman bound [24]) and hence must be dual to a CFT operator of dimension 3 or 1, built from hyper fields. The only such unitary operator is a fermion bilinear. AdS/CFT then states that the source for the dual operator (the fermion mass) and the value of the chiral condensate can be extracted from the asymptotic expansion of the scalar. These statements are made precise in section 3.3.

Our goal is thus to map the phase diagram of this $\mathcal{N} = 2$, non-conformal theory in the plane of mass versus temperature using this chiral condensate as our order parameter. In what sense is this chiral condensate an order parameter, however? That is, what are the

symmetries of our theory and what symmetry breaking does this order parameter detect?

$\mathcal{N} = 4$ SYM has an $SU(4) \simeq SO(6)$ R-symmetry. The hypers break the R-symmetry to $SO(4) \times SO(2)$. This is easy to see on the gravity side: the D7 wraps an S^3 inside the S^5 , breaking the $SO(6)$ isometry to the $SO(4)$ of the S^3 and an $SO(2)$. This $SO(2) \simeq U(1)$ is a chiral symmetry in that the hyper fermions, which have opposite chirality, carry opposite charges under it. With N_f flavors, the theory has in total a global $U(N_f) \times SO(2)_R \simeq SU(N_f) \times U(1)_B \times U(1)_A$. The $U(1)_A$ is our chiral symmetry in this case. At finite N_c , this $U(1)_A$ would be anomalous but as in large- N_c QCD the axial anomaly is suppressed as $N_c \rightarrow \infty$. Without the Yukawa interactions required by $\mathcal{N} = 2$ supersymmetry the $U(N_f)$ global symmetry would be enhanced to a $U(N_f)_L \times U(N_f)_R$.

In this paper, we consider only $N_f = 1$. This poses no problem on the gravity side: for this system, at zero mass, the factor of N_f would simply appear in front of the D7 action and would not affect the equations of motion³. These statements remain true at nonzero mass so long as all the flavor branes end at the same radius. A construction with different D7's ending at different radial values is possible, where the details of the spectrum would fix what remains of the $U(N_f)$, but we will not consider such a situation here (though it would be a straightforward extension).

3 The Probe Brane Action

3.1 Fefferman-Graham Coordinates

We will now write the action for the D7 slipping mode and show how to extract the mass and chiral condensate from solutions of the equation of motion (EOM). We also describe the boundary conditions in detail as these are somewhat different from those in [17, 18]. In these references and in much of the literature, a shooting method is employed, which is appropriate given only UV, or boundary, data. We impose boundary conditions in the IR, which is much simpler for numerics. In section 4 we will show that our IR boundary conditions reproduce the results of [17, 18] for the flat case. Boundary conditions similar to ours were used recently in [22] and also reproduced these results.

In units where we set the curvature radius L to one the AdS_5 metric in global coordinates has the form

$$ds^2 = G_{AB}dx^A dx^B = \frac{dr^2}{f(r)} + f(r)d\tau^2 + r^2 d\Omega_3^2 \quad (3.2)$$

³One subtlety that would however be present for $N_f \geq 2$ is that the configuration of lowest free energy might be found on the Higgs branch [19]. For $N_f = 1$ there is no Higgs branch since all hyper scalars have a quartic potential.

$$f(r) = \begin{cases} 1 + r^2 & \text{thermal AdS} \\ 1 + r^2 - \frac{M^2}{r^2} & \text{AdS-Schwarzschild} \end{cases} \quad (3.3)$$

$d\Omega_p^2$ is the standard metric for a p -sphere. Here the time coordinate τ has Euclidean signature and is periodic with period $2\pi T$ for temperature T . The parameter M is related to the black hole mass m_{bh} as $M = \frac{8G_N}{3\pi}m_{bh}$ and to the temperature as $M = \pi T$. For AdS-Schwarzschild, the horizon is at r_+ , the largest solution to the equation $f(r_+) = 0$. The flat case is the same with no 1 in $f(r)$ and with Euclidean 3-space instead of the S^3 .

In the above coordinates, the boundary is at $r \rightarrow \infty$. This makes extracting asymptotics from numerics difficult. These coordinates are also not well-suited to holographic renormalization. We thus switch to a Fefferman-Graham [25] coordinate system, where the metric takes the form

$$ds^2 = \frac{dz^2}{z^2} + \frac{1}{z^2}g_{ij}(z, \vec{x}, M)dx^i dx^j \quad (3.4)$$

$$g_{ij}(z, \vec{x}, M)dx^i dx^j = \frac{1}{4}(1 - z^4(1 + 4M^4))^2 F(z, M)^{-1} d\tau^2 + \frac{1}{4}F(z, M)d\Omega_3^2 \quad (3.5)$$

$$F(z, M) = 1 - 2z^2 + z^4(1 + 4M^4) \quad (3.6)$$

with radial coordinate z and $S^1 \times S^3$ coordinates x^i . The boundary is now at $z = 0$ and the horizon is at $z_+ = (1 + 4M^4)^{-1/4}$. Taking $M = 0$ gives g_{ij} for thermal AdS with center at $z = 1$. Notice also that in our conventions our boundary S^3 has radius 1/2.

The metric on the slice has an asymptotic expansion

$$g_{ij}(z, \vec{x}, M) = g_{ij}^0 + g_{ij}^2 z^2 + g_{ij}^4 z^4 + O(z^6) \quad (3.7)$$

$$g_{ij}^0 = \frac{1}{4}diag(1, S^3) \quad (3.8)$$

$$g_{ij}^2 = -\frac{1}{2}diag(-1, S^3) \quad (3.9)$$

$$g_{ij}^4 = \frac{1}{4}diag(1 - 12M^4, (1 + 4M^4)S^3) \quad (3.10)$$

where “ S^3 ” denotes the S^3 metric components. The S^5 metric is

$$d\Omega_5^2 = d\theta^2 + \sin^2 \theta d\psi^2 + \cos^2 \theta d\Omega_3^2 \quad (3.11)$$

The D7 then wraps the whole of AdS_5 and the S^3 inside the S^5 . The D7 slipping mode is the worldvolume scalar field $\theta = \theta(z)$, which is a function only of the radial coordinate to

preserve the Lorentz invariance of the boundary theory. If $\theta(z_0) = \frac{\pi}{2}$ for some finite z_0 , then the S^3 has “slipped off” the S^5 .

The D7 action is the Dirac-Born-Infeld (DBI) action, which in this background is simply the volume of the probe brane:

$$S_{D7} = T_{D7} \int d^8\xi \sqrt{\det P[G]} \quad (3.12)$$

where $P[G]$ is the pullback of the spacetime metric. With the $\theta(z)$ ansatz, the relevant part of the action is

$$S_{D7} = \int dz \frac{1}{16} \frac{1}{z^5} F(z, M) (1 - z^4(1 + 4M^4)) \cos^3 \theta(z) \sqrt{1 + z^2 \theta'(z)^2} \quad (3.13)$$

Again thermal AdS is the same with $M = 0$. Our objective is to solve the $\theta(z)$ EOM. We show in section 3.3 how to extract the mass and chiral condensate from a solution and in section 3.4 we explain the boundary conditions we impose on solutions.

3.2 Operator normalization

While we have already identified the operator dual to the slipping mode θ as the dimension 3 fermion bilinear, there is still some freedom in the overall normalization. Performing the integral over the S^3 in the 7-brane action gives a 5d action with prefactor

$$\frac{1}{g_5^2} = T_{D7} V_{S^3} = \frac{N_f}{g_s 2\pi^7 (\alpha')^4} (2\pi^2) = \frac{\lambda N_c N_f}{(2\pi)^4}. \quad (3.14)$$

where we used that in our $L = 1$ units $(\alpha')^{-2} = \lambda = g_{YM}^2 N_c = 4\pi g_s N_c$. According to the AdS/CFT dictionary the dual operator O has a 2-pt function

$$\langle O(x) O(0) \rangle = \frac{1}{g_5^2} \frac{2\Delta - d}{\pi^{d/2}} \frac{\Gamma(\Delta)}{\Gamma(\Delta - d/2)} \frac{1}{x^{2\Delta}} = \frac{\lambda N_c N_f}{4\pi^6} \frac{1}{x^6}. \quad (3.15)$$

In the field theory we are interested in the source term (the mass) and a vacuum expectation value for the operator $\tilde{O} = \bar{\lambda}\lambda$ where λ is a canonically normalized scalar. So far we have only established that $O = C\tilde{O}$ for some normalization constant C , but in order to interpret our results in the field theory we need to know C . One way to fix C is to compare the two point functions of O and \tilde{O} . Since \tilde{O} is a protected operator, its 2-pt function can be evaluated in the free theory. For a canonically-normalized fermion the position space propagator is simply $\langle \bar{\lambda}(x)\lambda(0) \rangle = \frac{1}{2\pi^2} \frac{\not{x}}{x^4}$ times flavor and color delta functions. So in the free theory we then simply get from Wick contractions

$$\langle \tilde{O}(x)\tilde{O}(0) \rangle = \frac{N_f N_c}{(2\pi^2)^2} \frac{\text{Tr}(\not{x}\not{x})}{x^8} = \frac{N_f N_c}{\pi^4} \frac{1}{x^6} \quad (3.16)$$

From which we can conclude that

$$O = \frac{\sqrt{\lambda}}{2\pi} \tilde{O}. \quad (3.17)$$

From this relation it becomes clear that all masses and condensates we find in this paper have to be multiplied by $\frac{\sqrt{\lambda}}{2\pi}$ to translate into field theory units. The phase transitions we study will happen at masses of order $\sqrt{\lambda}T$. This is the natural scale since the mesons in the theory only have masses of order $\frac{m}{\sqrt{\lambda}}$ [26]. At zero temperature the mass we obtain this way also agrees with the energy of a straight string stretching from the horizon to the flavor brane.

Note that the scaling of $\frac{1}{g_5^2}$ with N_f and N_c is expected simply from large N_c counting rules. The factor of λ however is a little surprising at first sight. Besides its effect on the normalization of the operators it will for example lead to free energies proportional to λ at large λ , indicating that in addition to the free value there is a 1-loop quantum correction but no further contributions from higher loops.

3.3 Holographic Renormalization and Free Energy

Given a solution of the EOM we need to extract the hyper mass and the chiral condensate. We use the method of holographic renormalization (which we call “holo-rg”) to do this as well as compute the on-shell action. We will now briefly review the holo-rg procedure [27, 28, 29, 30].

The precise statement of AdS/CFT equates the 10D on-shell SUGRA action with the generating functional of the boundary field theory. The leading asymptotic value of a bulk field serves as a source for the corresponding field theory operator, i.e. derivatives of the SUGRA action w.r.t. leading asymptotic values will give boundary correlators. This will be made explicit for our $\theta(z)$ field below.

Both the SUGRA action and the field theory generating functional are formally infinite: the SUGRA action suffers IR divergences while the field theory has UV divergences. Holo-rg proceeds first by regulating the SUGRA action. This means integrating, not to the $z = 0$ boundary, but only to $z = \epsilon$. Local, covariant counterterms are then added on the $z = \epsilon$ slice, built from the metric induced on the slice, γ_{ij} , curvature invariants thereof and fields on the slice, for instance our $\theta(\epsilon)$. The coefficients of these counterterms are fixed by requiring all divergences to cancel. Functional derivatives w.r.t. asymptotic values can then be taken, followed by removal of the regulator, $\epsilon \rightarrow 0$, yielding renormalized boundary correlators. Covariance and all other symmetries can be maintained throughout this procedure. Holo-rg also gives us a way to compute a renormalized free energy of our $\mathcal{N} = 2$ theory, since via AdS/CFT this is just equivalent to the on-shell SUGRA action. We find this much more elegant, in principle and in practice, than a background subtraction technique.

Now to make all of this explicit for our system. The holo-rg procedure for precisely this system, a probe D7 in $AdS_5 \times S^5$, was worked out in [31], so we quote those results. According to the AdS/CFT dictionary, the mass and condensate for the hyper fermions come from the asymptotic expansion

$$\theta(z) = \theta_0 z + \theta_2 z^3 + \Theta_2 z^3 \log z + \dots \quad (3.18)$$

where the mass will be given by θ_0 and the condensate will be fixed by θ_0 and θ_2 . In this case, the log coefficient $\Theta_2 = 2\theta_0$ [31]. The counterterms for this system are given in [31]⁴. We include a second finite counterterm, L_{f2} :

$$L_1 = -\frac{1}{4}\sqrt{\gamma} \quad (3.19)$$

$$L_2 = \frac{1}{48}\sqrt{\gamma}R_\gamma \quad (3.20)$$

$$L_3 = -\log(\epsilon)\sqrt{\gamma}\frac{1}{32}(R_{ij}R^{ij} - \frac{1}{3}R_\gamma^2) \quad (3.21)$$

$$L_4 = \frac{1}{2}\sqrt{\gamma}\theta^2(\epsilon) \quad (3.22)$$

$$L_5 = \frac{1}{12}\log(\epsilon)\sqrt{\gamma}R_\gamma\theta(\epsilon)^2 \quad (3.23)$$

$$L_{f1} = -\frac{5}{12}\sqrt{\gamma}\theta(\epsilon)^4 \quad (3.24)$$

$$L_{f2} = \frac{1}{6}\sqrt{\gamma}R_\gamma\theta(\epsilon)^2 \quad (3.25)$$

$$(3.26)$$

We will denote the subtracted action as $S_{sub} = S_{D7} + \sum_i L_i$ and the renormalized action as $S_{ren} = \lim_{\epsilon \rightarrow 0} S_{sub}$. Notice that $\sqrt{\gamma} = \epsilon^{-4}\sqrt{g}$ and $R_\gamma = \epsilon^2 R_g$ and to leading order $\theta(\epsilon) \sim \theta_0 \epsilon$, so the last two counterterms are finite. The first three counterterms are needed to renormalize the volume of AdS_5 . The divergent piece of L_3 has coefficient $R_{ij}^0 R_0^{ij} - \frac{1}{3}R_0^2$. For our g_{ij}^0 , this quantity vanishes and hence L_3 is not needed. L_4 and L_5 are the counterterms for a free scalar in AdS_5 . The coefficient of L_{f1} is fixed by requiring a supersymmetric renormalization scheme [31]. The condensate is given by

$$\langle \bar{q}q \rangle = \lim_{\epsilon \rightarrow 0} \frac{1}{\epsilon^3} \frac{\delta S_{sub}}{\sqrt{\gamma} \delta \theta(\epsilon)}. \quad (3.27)$$

Without counterterm L_{f2} this would be [31]

⁴This reference used a convention that AdS space had constant *positive* curvature. We use the opposite convention, hence our counterterms have $R_\gamma \rightarrow -R_\gamma$ relative to those in [31].

$$\langle \bar{q}q \rangle = -2\theta_2 + \frac{1}{3}\theta_0^3 - \frac{1}{12}R_0\theta_0 \quad (3.28)$$

We included L_{f2} but found no holo-rg scheme to fix its coefficient. A natural choice would be to fix the coefficient to cancel the R_0 term in the condensate. This coefficient would be $1/24$. We found numerically that a value three to four times this gave plots for the curved case that, to the naked eye, were more similar to those for flat case except for large mass (as explained in section 5). We therefore used a coefficient of $1/6$ in the plots that appear in our figures. We verified that our results for the existence of a first-order transition and the value of the mass at which the transition occurs are independent of the choice of L_{f2} 's coefficient. In short, while our plots are scheme-dependent our final answer for the phase diagram is not.

The free energy of the field theory is given by the on-shell value of the renormalized action. The order N_c^2 contribution to the free energy comes from the 10d SUGRA action and is untouched by the introduction of the probe brane. Naively there are two sources of order $N_f N_c$ corrections, the renormalized value of the on-shell DBI action as well as the order $\frac{N_f}{N_c}$ correction to the order N_c^2 on-shell bulk SUGRA action due to the backreaction. The latter however is proportional to the variation of the supergravity action with respect to the unperturbed background metric and hence vanishes. The backreaction only enters at order N_c^0 and the only order $N_f N_c$ contribution to the free energy comes from the renormalized on-shell DBI action.

In summary, our procedure is this: solve the EOM for $\theta(z)$ (with the boundary conditions explained in the next section). With this solution, we can immediately find the mass and condensate for that value of z_0 . We also plug this solution into S_{ren} to find the free energy. We can then go to the next value of z_0 , which amounts to dialing the mass. In this fashion, from the behavior of the condensate and the free energy, we can identify the chiral phase transition and determine its order.

3.4 Boundary Conditions

We will discuss first the $M = 0$ thermal AdS case, with no black hole horizon. We consider two kinds of solutions. The first kind are D7's ending at some finite z_0 , i.e. $\theta(z_0) = \pi/2$. This is our first boundary condition, and we want a second condition in the IR. We find one by requiring that the D7 ends smoothly, with no conical deficit. The pulled-back D7 metric contains terms

$$ds_{D7}^2 \supset \left(\frac{1}{z^2} + \theta'(z)^2\right) dz^2 + \cos^2 \theta(z) d\Omega_3^2 \quad (3.29)$$

Let $\alpha = \cos \theta(z)$ so that $d\alpha = -\sin \theta(z)\theta'(z)$ and hence

$$ds_{D7}^2 \supset \frac{(\frac{1}{z^2} + \theta'(z)^2)}{\theta'(z)^2 \sin^2 \theta} d\alpha^2 + \alpha^2 d\Omega_3^2 \quad (3.30)$$

No conical deficit means the coefficient of $d\alpha^2$ must be one when $z = z_0$. This gives $z_0^{-2}\theta'(z_0)^{-2} = 0$ and hence $\theta'(z_0) = \infty$. We implement this numerically with a number on the order of 10^3 .

The second kind of solution is for D7's extending to the center of AdS at $z_0 = 1$. In this case, we choose a boundary condition $\theta(z = 1) = \beta$ for some angle $0 \leq \beta \leq \pi/2$. $\beta = 0$ is the massless case and dialing β will interpolate smoothly to a D7 ending precisely at the center. The second boundary condition is now the Neumann condition $\theta'(z = 1) = 0$.

In AdS-Schwarzschild we also have two kinds of solutions, D7's ending outside the horizon or ending on the horizon. For D7's ending outside the horizon we use the same boundary conditions as those in thermal AdS. For D7's ending on the horizon we use boundary conditions $\theta(z_+) = \beta$ and $\theta'(z_+) = 0$. The flat case, where the horizon is present for any finite temperature, also has these two types of solutions with these boundary conditions.

In much of the literature (for example [17, 18, 32]), IR boundary information such as this is not used. Instead, a shooting method is used. To justify and cross-check our method, in the next section we will reproduce some known results for the flat case using our boundary conditions and holo-rg. We will also compare our curved case results in the high-temperature limit to these results as a useful check.

4 The Flat Case

The thermodynamics of this $\mathcal{N} = 2$ theory has been studied in [17, 18]. We will compute the chiral condensate as a function of the mass, the free energy as a function of the mass and then draw the phase diagram. As suggested in [17, 18], a first-order phase transition does occur at a critical value of the mass. The critical value is $m_{crit} \approx 1.30$ (for $M = 1$)⁵. The form of the free energy shows this clearly. In this case, our AdS_5 metric is

$$ds^2 = \frac{dz^2}{z^2} + \frac{1}{z^2} \frac{1}{2} (1 - z^4 M^4)^2 F(z, M)^{-1} d\tau^2 + \frac{1}{z^2} \frac{1}{2} F(z, M) d\vec{x}^2 \quad (4.31)$$

$$F(z, M) = 1 + z^4 M^4 \quad (4.32)$$

and the horizon is at $z_+ = 1/M$. An important fact we will need later is that the last term in the metric has a $1/2$ whereas the curved case metric had a $1/4$, hence z in the flat case

⁵Our m_{crit} is larger than the $m_{crit} \approx 0.92$ in [17, 18, 22] by a factor of $\sqrt{2}$. This comes from our choice of coordinates. The coordinate r in [22] is related to our z by $z = \frac{1}{\sqrt{2}} \frac{1}{r}$. We verified that this change of coordinates reproduces fig. 2(b) of [22].

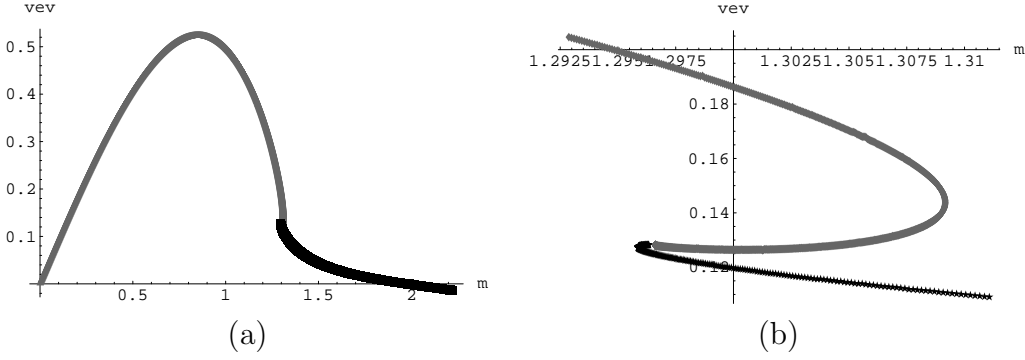


Figure 3: (a.) Chiral Condensate as a function of mass ($M = 1$); gray and black curves indicate solutions ending inside and outside the horizon respectively (b.) Close-up view of (a.)

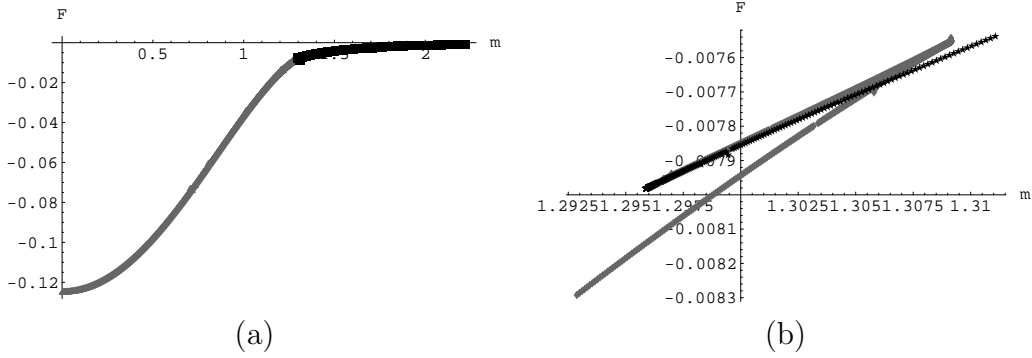


Figure 4: (a.) Free Energy as a function of mass ($M = 1$). (b.) Close-up view of (a.)

is $\sim \sqrt{2}z$ in the curved case and the mass we extract from eq. 3.18 in the flat case will thus be $1/\sqrt{2}$ times the mass we compute in the curved case. This is important when comparing the phase diagrams in the two cases, in particular their slope, as we do in section 5.

The D7 action is now

$$S_{D7} = \int dz \frac{1}{4} \frac{1}{z^5} (1 - z^8 M^8) \cos^3 \theta(z) \sqrt{1 + z^2 \theta'(z)^2}. \quad (4.33)$$

The counterterms are given above but with $L_2 = L_3 = L_5 = L_{f2} = 0$ because $R_\gamma = 0$.

Our results for the condensate are summarized in figure (3) and for the free energy in (4), clearly reproducing the first order phase transition found in earlier work. The condensate as a function of mass is multivalued; the plot of the free energy shows that at a critical value of the mass we discontinuously jump from a D7 ending some finite distance away from the horizon to a D7 touching the horizon. In terms of the induced metric on the worldvolume of the D7 brane this transition corresponds to a topology-changing phase transition.

The phase diagram for this theory appears in figure (5). As explained in the introduction,

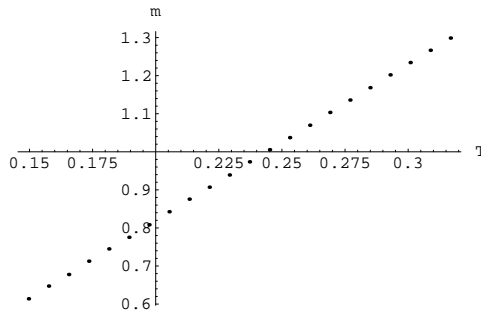


Figure 5: Phase Diagram of the $\mathcal{N} = 2$ theory in flat space. $T = M/\pi$.

this is a straight line. A linear fit to this data gives a slope of ≈ 4.1 and a y-intercept of zero. This is expected since in a conformal theory two scales are needed for a transition and either T or m going to zero eliminates one scale.

5 The Curved Case

We start with thermal AdS, for temperatures below T_{HP} . We find a surprise. In terms of the topology of the D7 brane there are still two classes of solutions: the D7 brane can either end at a finite value of the radial coordinate and hence have a finite size S^3 inside the AdS_5 , or it can reach all the way to the center of AdS_5 with this time the S^3 inside the S^5 remaining finite. The two branches meet at the point where both S^3 's shrink at the center of AdS. In the field theory we expect the two configurations to correspond to a competition between the explicit mass terms we added for the hypers with the curvature induced scalar masses. Figure (6) shows our results for the vev and figure (7) shows the free energy. Neither the free energy nor the condensate is multiple-valued in the mass. We conclude that the topology change in the bulk goes unnoticed in the dual field theory. In other words, despite the topology-changing transition in the bulk we find no first-order transition in the field theory.

At large mass the finite volume effects should be negligible and we should recover the zero temperature flat space results, that is the leading piece in both vev and free energy vanish. Writing the vev as a power series

$$\langle O \rangle = m^3 \left(o_0 + o_1 \frac{1}{mR_3} + o_2 \frac{1}{(mR_3)^2} + o_3 \frac{1}{(mR_3)^3} + \dots \right) \quad (5.34)$$

the large-mass limit tells us that $o_0 = 0$. o_2 can be set to zero by appropriate choice of the finite counterterm L_{f2} . Note that the subleading $\langle O \rangle = o_1 \frac{m^2}{R_3}$ leads to a vev that is growing at large mass for any finite R_3 as we do also see in our numerics.

Also note that our free energy has a non-vanishing positive value of $0.09 \approx 3/32$ at zero temperature. This can be interpreted as the $\lambda N_f N_c$ contribution to the Casimir energy of

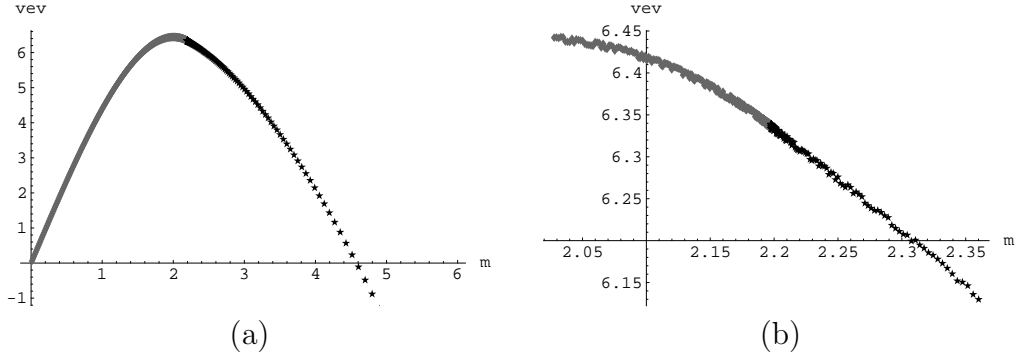


Figure 6: (a.) Thermal AdS chiral condensate as a function of mass. Gray curves are branes ending at the center of AdS, black is ending at finite $z < 1$ (b.) Close-up of (a.)

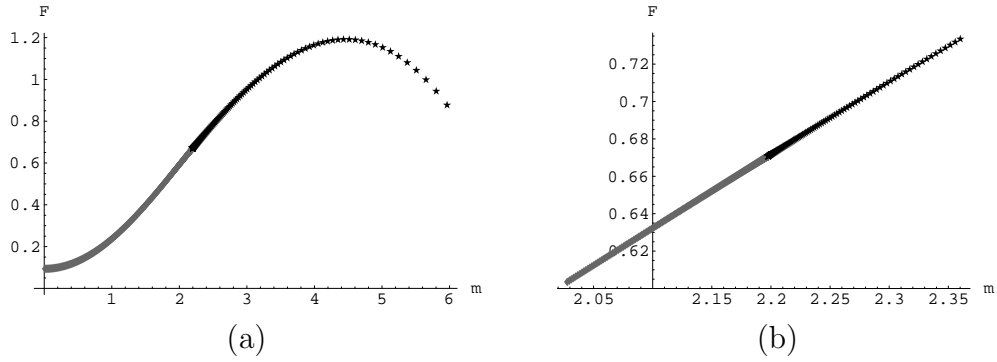


Figure 7: (a.) Thermal AdS free energy as a function of mass. (b.) Close-up of (a.)

the system on the sphere. In the massless case the solution can even be obtained analytically, $\theta(z) = 0$, and we get an analytic expression for the DBI contribution to the Casimir energy,

$$E_{C,N_c} = \frac{V}{g_5^2} \frac{3}{32} = \frac{3\lambda N_f N_c}{2^9 \pi^4} V \quad (5.35)$$

where V denotes the volume of the 3-sphere. The leading order (in N_c) contribution to the Casimir energy comes purely from the supergravity action evaluated on background $\text{AdS}_5 \times S^5$ geometry itself and has been obtained in [29],

$$E_{C,N_c^2} = \frac{3N_c^2}{32\pi^2} V. \quad (5.36)$$

Their result matches perfectly the free field theory result, where one basically just counts the number of fields and hence gets a contribution of order N_c^2 from the adjoint fields with no powers of λ . This agreement is guaranteed by supersymmetry. In [33, 34] it was shown that the Casimir energy can be obtained from the conformal anomaly by exploiting the fact that the sphere is conformal to flat space and the latter is assigned zero Casimir energy. The conformal anomaly however is completely protected (that is, independent of the coupling constant) in a theory with at least $\mathcal{N} = 2$ supersymmetry⁶ and hence so is the Casimir energy on the sphere (or any other space conformal to flat space).

The order $N_f N_c$ correction we found to this leading order Casimir energy is proportional to λ and hence can not possibly match the free field value, but rather seems to come from a 1-loop contribution with no higher-loop corrections. Since we do have $\mathcal{N} = 2$ supersymmetry preserved the conformal anomaly should still be protected⁷. However, this time there is an additional contribution to $\langle T_\mu^\mu \rangle$ from the scale anomaly due to the non-vanishing beta function. In an $\mathcal{N} = 2$ theory the beta-function is 1-loop exact and this relation hence explains why at strong coupling we only see the order λ correction and no higher powers of λ . Our result seems to indicate that the Casimir energy in a similar fashion only gets a contribution from 1-loop. It would be interesting to see if this can be verified from a weak coupling calculation.

Finally we come to the AdS-Schwarzschild case for $T > T_{HP}$. We find that for $T \gtrsim 10 * T_{HP}$ the free energy and condensate already have nearly the same form as the flat case in figures (3) and (4). As T decreases, these continuously deform to the shapes shown in figures (8) and (9) where $T = 1.75 * T_{HP}$. In close-up we find that the condensate is again double-valued

⁶With $\mathcal{N} = 1$, supersymmetry still relates the conformal anomaly to a protected R-current anomaly, but different U(1)s can play the role of the superconformal R-current at different values of the coupling.

⁷Indeed it was shown in [35] that in a closely related system with an O7 in addition to 4 probe D7s the supergravity anomaly perfectly reproduces the field theory anomaly. It is easy to see that without the orientifold their analysis for a single D7 reproduces the right value corresponding to a fundamental hyper. In their case the field theory was exactly conformal (not just to leading order in $\frac{N_f}{N_c}$) and in the bulk the order $\lambda N_f N_c$ contribution to the Casimir energy canceled between the orientifold and D7s

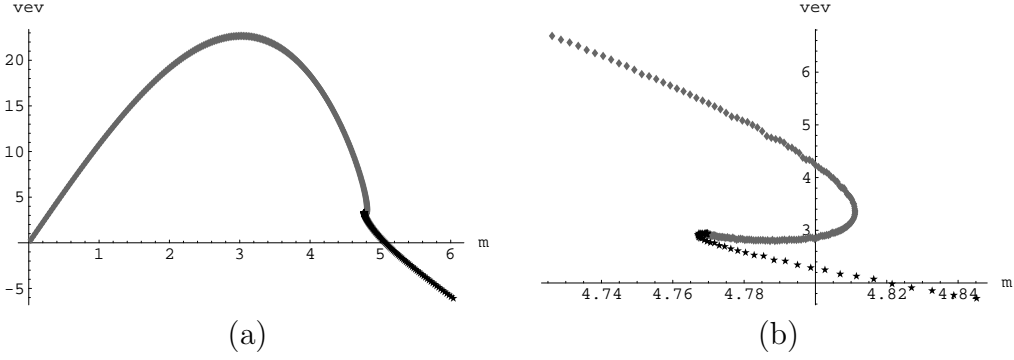


Figure 8: (a.) AdS-Schwarzschild chiral condensate as a function of mass. Gray curves are branes falling into the horizon, black is ending outside. $T = 1.75 * T_{HP}$ (b.) Close-up of (a.)

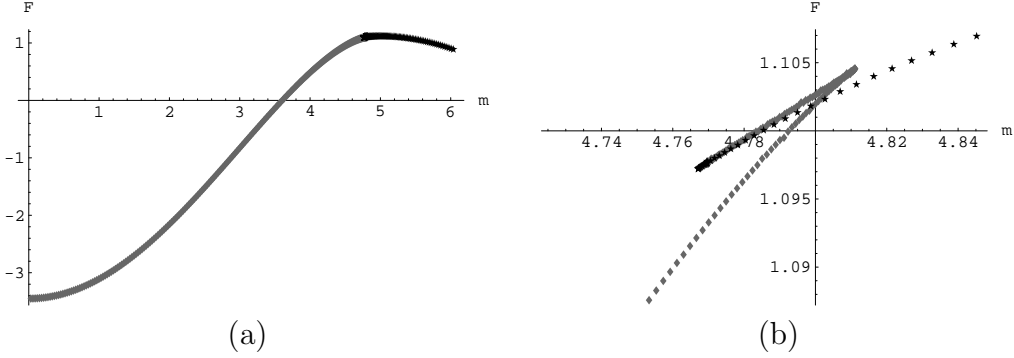


Figure 9: (a.) AdS-Schwarzschild free energy as a function of mass. $T = 1.75 * T_{HP}$ (b.) Close-up of (a.)

and will jump discontinuously. The free energy again has a discontinuous first derivative just as in the flat case. This remains true all the way down to T_{HP} so no critical point analogous to the point C in the large- N_c QCD phase diagram appears for this theory.

Putting both the high temperature and low temperature regions together we finally arrive at the phase diagram for our theory, as displayed in figure (2). No first-order transition occurs below the $T = T_{HP}$ vertical deconfinement transition line. A linear fit indicates that the chiral transition line has slope ≈ 5.8 . This agrees with the earlier result of 4.1 from the flat case after taking into account the factor of $\sqrt{2}$ difference between the z coordinate of our flat-case metric and that of our AdS-Schwarzschild metric: $5.8 \approx \sqrt{2} * 4.1$. The chiral transition line intercepts the deconfinement line at $m \approx 2.6$.

6 Conclusion

We have presented a numerically-generated phase diagram for large- N_c $\mathcal{N} = 4$ super-Yang-Mills on a 3-sphere coupled to N_f massive fundamental hypers, including the first-order chiral phase transition line. Below the Hawking-Page temperature we find that, despite a topology-changing transition in the bulk, a first-order transition does not occur in the boundary theory.

Isospin chemical potential could be included in this analysis by introducing multiple D7's ending at different values of the AdS radius, allowing for 7-7 strings and hence heavy-light mesons. Baryon number chemical potential could be included by turning on the gauge potential on the D7 worldvolume, although it is unclear what boundary conditions to impose on this field in the IR. Supposing that question could be answered, this would be one advantage AdS/CFT would have over lattice gauge theory which currently cannot easily include baryon number chemical potential. Other interesting extensions include studying the corresponding phase diagram at weak coupling and studying the effects of the D7 backreaction.

Acknowledgements

We would like to thank C.R. Graham, C. Herzog, D. Mateos, S. Sharpe, K. Skenderis, M. Strassler, and L. Yaffe for helpful discussions. A. O'B. would also like to thank D. Yamada. The work of A.K. was supported in part by DOE contract # DE-FG02-96-ER40956. The work of A. O'B. was supported by a Jack Kent Cooke Foundation scholarship.

References

- [1] J. M. Maldacena, *Adv. Theor. Math. Phys.* **2**, 231 (1998) [*Int. J. Theor. Phys.* **38**, 1113 (1999)] [arXiv:hep-th/9711200].
- [2] E. Witten, *Adv. Theor. Math. Phys.* **2**, 505 (1998) [arXiv:hep-th/9803131].
- [3] B. Sundborg, *Nucl. Phys. B* **573**, 349 (2000) [arXiv:hep-th/9908001].
- [4] O. Aharony, J. Marsano, S. Minwalla, K. Papadodimas and M. Van Raamsdonk, *Adv. Theor. Math. Phys.* **8**, 603 (2004) [arXiv:hep-th/0310285].
- [5] A. Karch and E. Katz, *JHEP* **0206**, 043 (2002) [arXiv:hep-th/0205236].
- [6] R. D. Pisarski and F. Wilczek, *Phys. Rev. D* **29**, 338 (1984).
- [7] F. Wilczek, *Nucl. Phys. A* **566**, 123C (1994) [arXiv:hep-ph/9308341].

- [8] F. Wilczek, Int. J. Mod. Phys. A **7**, 3911 (1992) [Erratum-ibid. A **7**, 6951 (1992)].
- [9] F. Karsch and E. Laermann, Phys. Rev. D **50**, 6954 (1994) [arXiv:hep-lat/9406008].
- [10] M. D'Elia, A. Di Giacomo and C. Pica, PoS **LAT2005**, 158 (2005) [arXiv:hep-lat/0510012].
- [11] G. Boyd, J. Fingberg, F. Karsch, L. Karkkainen and B. Petersson, Nucl. Phys. B **376**, 199 (1992).
- [12] R. D. Pisarski, arXiv:hep-ph/9503330.
- [13] F. Neri and A. Gocksch, Phys. Rev. D **28**, 3147 (1983).
- [14] R. D. Pisarski, Phys. Rev. D **29**, 1222 (1984).
- [15] O. Aharony, J. Marsano, S. Minwalla, K. Papadodimas and M. Van Raamsdonk, Phys. Rev. D **71**, 125018 (2005) [arXiv:hep-th/0502149].
- [16] H. J. Schnitzer, Nucl. Phys. B **695**, 267 (2004) [arXiv:hep-th/0402219].
- [17] J. Babington, J. Erdmenger, N. J. Evans, Z. Guralnik and I. Kirsch, Phys. Rev. D **69**, 066007 (2004) [arXiv:hep-th/0306018].
- [18] I. Kirsch, Fortsch. Phys. **52**, 727 (2004) [arXiv:hep-th/0406274].
- [19] R. Apreda, J. Erdmenger, N. Evans and Z. Guralnik, Phys. Rev. D **71**, 126002 (2005) [arXiv:hep-th/0504151].
- [20] M. Kruczenski, D. Mateos, R. C. Myers and D. J. Winters, JHEP **0405**, 041 (2004) [arXiv:hep-th/0311270].
- [21] D. Mateos, R. C. Myers and R. M. Thomson, arXiv:hep-th/0605046.
- [22] T. Albash, V. Filev, C. V. Johnson and A. Kundu, arXiv:hep-th/0605088.
- [23] S. W. Hawking and D. N. Page, Commun. Math. Phys. **87**, 577 (1983).
- [24] P. Breitenlohner and D. Z. Freedman, Annals Phys. **144**, 249 (1982).
- [25] C. Fefferman and C. Robin Graham, 'Conformal Invariants,' in *Elie Cartan et les Mathematiques d'aujourd'hui* (Asterisque, 1985) 95.
- [26] M. Kruczenski, D. Mateos, R. C. Myers and D. J. Winters, JHEP **0307**, 049 (2003) [arXiv:hep-th/0304032].
- [27] M. Henningson and K. Skenderis, JHEP **9807**, 023 (1998) [arXiv:hep-th/9806087].

- [28] M. Henningson and K. Skenderis, *Fortsch. Phys.* **48**, 125 (2000) [arXiv:hep-th/9812032].
- [29] V. Balasubramanian and P. Kraus, *Commun. Math. Phys.* **208**, 413 (1999) [arXiv:hep-th/9902121].
- [30] S. de Haro, S. N. Solodukhin and K. Skenderis, *Commun. Math. Phys.* **217**, 595 (2001) [arXiv:hep-th/0002230].
- [31] A. Karch, A. O’Bannon and K. Skenderis, arXiv:hep-th/0512125.
- [32] N. J. Evans and J. P. Shock, *Phys. Rev. D* **70**, 046002 (2004) [arXiv:hep-th/0403279].
- [33] A. Cappelli and A. Coste, *Nucl. Phys. B* **314**, 707 (1989).
- [34] K. Skenderis, *Int. J. Mod. Phys. A* **16**, 740 (2001) [arXiv:hep-th/0010138].
- [35] O. Aharony, J. Pawelczyk, S. Theisen and S. Yankielowicz, *Phys. Rev. D* **60**, 066001 (1999) [arXiv:hep-th/9901134].